AN X-RAY SPECTROMETER DETERMINATION OF RETAINED AUSTENITE IN STEEL

by

Walter Edward Littmann

B.S., in Metallurgical Engineering, University of Cincinnati

(1950)

SUBMITTED IN PARTIAL FULFILLMENT OF THE
REQUIREMENTS FOR THE DEGREE OF
MASTER OF SCIENCE

at the

MASSACHUSETTS INSTITUTE OF TECHNOLOGY

(1952)

Signature of Author .....
Department of Metallurgy, May 16, 1952

Certified by .....
Thesis Supervisor

.....
Chairman, Departmental Committee on Graduate Students

AUG 28 1952
LIBRARY

ABSTRACT

AN X-RAY SPECTROMETER DETERMINATION OF RETAINED AUSTENITE IN STEEL

by

Walter Edward Littmann

Submitted to the Department of Metallurgy on May 16, 1952 in partial fulfillment of the requirements for the degree of Master of Science

The volume percentage of austenite retained in quench hardened S.A.E. 52100 and 1045 steels was determined by comparison of the x-ray diffraction line energies. The line energies were measured using a Geiger Counter high angle x-ray spectrometer by three methods, automatic recording on a chart, automatic integration using a mechanical counter, and point by point counting. The automatic recording of the diffraction lines on a chart was found to be the most reproducible method for a given time per determination.

Cobalt, iron and chromium radiations were used and compared. Inability to reduce iron fluorescence in the background seriously impaired the usefulness of cobalt and iron radiation in the method. The use of chromium radiation, however, when filtered with 0.001 inch vanadium foil permitted accurate determinations of retained austenite.

The results obtained by the x-ray method agreed with those from lineal analysis where the methods were mutually applicable.

The lowest austenite content measured was 3 percent but the lower limit of the method was estimated to be about 0.1 to 0.5 percent austenite depending on the stability of the x-ray tube power output and the time used for each determination.

The outstanding features of the method are its simplicity, the use of automatic equipment, and short times required for a single determination. The reproducibility of the method is proportional to the time used for each run. Accurate results can be obtained for a sample in one hour using the recorded pattern technique. For such a method, the result of a single determination will be within 1/2 - 2 percent of austenite of the true value depending on the stability of the tube output and the time used for each pattern. The time required for each determination is practically independent of the amount of austenite present.

Thesis Supervisor: John Wulff
Title: Professor of Metallurgy

TABLE OF CONTENTS

		Page
ABSTRACT		ii
LIST OF FIGURES		v
LIST OF TABLES		vii
ACKNOWLEDGEMENTS		viii
I	INTRODUCTION	1
II	THEORY	7
III	EXPERIMENTAL WORK	15
	A. Materials and Equipment	15
	B. Radiation and Filtering	23
	C. Effect of Grain Size and Preferred Orientation	33
	D. Operation and Integration	38
	E. Results	47
IV	DISCUSSION AND CONCLUSIONS	60
V	SUGGESTIONS FOR FUTURE WORK	63
VI	APPENDIX	64
VII	BIBLIOGRAPHY	68

LIST OF FIGURES

		Page
Figure 1	Recorded Patterns Showing Cementite Lines	
	(a) Spheroidized Steel A	13
	(b) Sample A-8 q	13
Figure 2	Arrangement of the Elements of the X-ray. Spectrometer Showing Focusing Conditions.	21
Figure 3	Comparison of Patterns of Sample A-6 q Made Using	
	(a) Iron Radiation Filtered with Manganese Oxide	26
	(b) Cobalt Radiation Filtered with Iron Foil	26
	(c) Chromium Radiation Filtered with Vanadium Foil	26
Figure 4	Effect of Filtering and Tube Voltage on Contrast	27
Figure 5	Arrangement of X-ray Source, Sample and Film for Front Reflection Films	34
Figure 6	Front Reflection Patterns Recorded on Films Using Unfiltered Cobalt Radiation..	35
Figure 7	Diffraction Lines Recorded Photographically at Spectrometer Focus	37
Figure 8	Methods 1 and 2 for Automatic Integration Illustrated Schematically	40

LIST OF FIGURES
(continued)

Page

Figure 9 Recorded Pattern of Sample A-7 q Showing Possible Interaction between γ(220) and α(211) 43

Figure 10 Recorded Pattern of Sample B-1 q Illustrating the Background Trend 45

Figure 11 Derivation of the Absorption Factor for the X-ray Spectrometer 67

LIST OF TABLES

		Page
I	Analyses of Steels Used	16
II	Sample Designations and Heat Treatments	16
III	Treatment of Specimens Subsequent to Hardening	19
IV	Effect of Filtering on Contrast between a Diffraction Line and Background	31
V	Effect of Erroneous Location of the Line Center on Results by Automatic Integration Using Method 1	42
VI	Comparison of Method 1 and Method 2	46
VII	Comparison of Percent Austenite from Lineal Analysis with X-ray Results	48
VIII	Tabulation of Results	49-52
IX	Comparison of Observed and Calculated Intensity Ratios for Lines from the Same Phase	54
X	Effect of Corrections for Tempering on the Results from Recorded Pattern 4	58
XI	Results with Cobalt Radiation	59

ACKNOWLEDGEMENTS

The author wishes to acknowledge with thanks the fellowship grant provided by the Timken Roller Bearing Co. and the advice of Professors Wulff, Norton and Rautala of the Department of Metallurgy.

I INTRODUCTION

The quantitative measurement of retained austenite contents in quench-hardened steels has become important since research has demonstrated some of the effects that retained austenite may have on the physical properties of such materials. Recently it has been shown that retained austenite is present in all quench-hardened carbon steels containing 0.20 percent carbon or more.(1)

The x-ray method is almost the only method independent of external calibration which permits quantitative measurement of the volume percentage of austenite in a given steel in the range of austenite contents below ten percent. The electron microscope is capable of resolving such amounts of austenite in a polished section but the accuracy of any such determination would depend on etching techniques. Surface preparation would be extremely important, and a long time would be required by a highly trained person to carry out a single determination.

The spectrometer technique provides a simple method for determining retained austenite contents

with accuracy at least equal to that of any other method in use at present. The simplicity of the method makes it ideal for routine determinations using automatic equipment, thus requiring a minimum expenditure of time for a given degree of accuracy.

An excellent summary of the work done on x-ray determinations of retained austenite prior to 1947 appeared in the Sc.D. thesis of Averbach[2] and in one of the publications by Averbach and Cohen based on that thesis.[3] The authors were the first to emphasize the importance of using the integrated line energy rather than the peak intensities when the ratio of austenite and martensite volumes present in a sample was to be determined by a comparison of the diffraction lines of the phases.

In the method of Averbach and Cohen the x-ray diffraction lines were recorded photographically in a Debye camera. Cobalt K radiation was obtained by diffraction of a collimated beam of cobalt radiation from the (200) planes of a flat rock salt crystal monochromator. The monochromated radiation irradiated a flat specimen placed at a grazing angle of 60 degrees, the following lines being thus recorded on the film:

Austenite, (220) and (311); Martensite, (200), (211), and (220). After photographic processing to give linear blackening, the films were microphotometered, and the integrated intensity obtained by a special integration of the area under peak above the background, the photometer traces being converted to blackening curves before measurement. A plot of these line energies, divided by appropriate factors, as a function of the Bragg angle, θ, showed the effect of absorption, since the total diffracting volume was not the same for all lines in the pattern. Two such plots were made, one for the austenite lines, the other for the martensite lines. The factor relating the two curves gave the ratio of austenite to martensite in the structure, permitting calculation of the percentages of each. The results thus obtained agreed with results obtained by lineal analysis(4) within the limits of experimental error, the reproducibility being somewhat better for the x-ray method.

The disadvantage of long exposure time was somewhat minimized later by the use of a bent and ground rock salt crystal monochromator(1). A divergent

beam was thus focussed on the entrance slit of a Debye camera, a divergent beam striking the specimen at a grazing angle of 60 degrees. A collimator was used inside the camera to limit the divergence of the beam and thus minimize line broadening, since focussing conditions could not be realized with such an arrangement. A technique involving duplicate exposures with the film masked in one case with aluminum foil permitted determination of austenite contents as small as 0.3 percent. Iron radiation was used on low austenite specimens of steels containing high manganese to minimize the fluorescence which made separation of the broad, weak austenite lines from the background difficult.

The outstanding advantage of the integrated intensity method is its high sensitivity in the low austenite range where no other method is available for determining quantitively the amount of retained austenite independent of external calibration. A disadvantage is still presented by the fact that the time required for a single determination by the photographic method is especially long when the amount of

retained austenite is less than 4 percent. Because blackening is not linearly proportional to intensity a special integration by Simpson's rule is required to determine each line energy.[5] Furthermore, the necessity of having more than a single pair of lines to minimize the errors in making the correction for absorption hinders the effective use of chromium radiation which separates the lines and permits more accurate determination of the background level. The use of chromium radiation is desirable especially when the specimen is a chromium steel because of fluorescence of chromium by any radiation of higher atomic number than itself. When chromium radiation was used on a 1% carbon, 5% chromium steel by Majer[6], difficulty was encountered in the microphotometering of the broad, very intense (211) martensite line, even though the specimens in his investigation were tempered 15 seconds at 600°F to permit comparison with lineal analysis. Such treatment removed much of the tetragonality from the martensite lines, making them somewhat sharper than in the as quenched condition.

In view of the disadvantages of the photographic method, it was felt that something might be gained by a modification of the technique for the use of the Geiger-Müller tube spectrometer where the intensity is measured directly.

II THEORY

A complete treatment of the theoretical aspects of the x-ray method for retained austenite determination was set forth in reference (2). Some simple simplifications have been made in this investigation and a brief review of the theoretical basis of the x-ray method is in order. Following much of the notation of Taylor[7] the total energy (integrated intensity) of a given diffraction line entering the window of a spectrometer Geiger tube is $E_{(hkl)}$. For the line (hkl) of phase , in a powder-type specimen, $E_{(hkl)}$ is given by the following equation:

Eq. (1)

$$E_{\alpha(hkl)} = \left[E_o \lambda^3 \left(\frac{e^2}{mc^2}\right)^2 \frac{1}{32\pi R}\right] pAe^{-2M} \left|F_{\alpha(hkl)}\right|^2 (L.P.) V_\alpha N_\alpha^2$$

where $E_{\alpha(hkl)}$ = Integrated intensity (total line energy) for a given α diffraction line (hkl)

E_o = incident intensity

λ = wave length of radiation being diffracted

$\dot{e}$ = charge on the electron

m = mass of the electron

c = velocity of light

l = height of receiving slit at Geiger tube

R = radius of spectrometer

p = multiplicity factor

A = absorption factor

e^{-2M} = Debye-Waller temperature factor

$F_{\alpha}(hkl)$ = structure factor per unit cell of phase α

L.P. = Lorentz and Polarization factor = $\frac{1+\cos^2 2\theta}{2\cos\theta\sin^2\theta}$

V_{α} = volume of α irradiated

N_{α} = number of unit cells of α per unit volume

$N_{\alpha} = \frac{1}{v_{\alpha}}$ where v_{α} = volume of unit cell of phase α

Since everything within the bracket in Equation (1) is constant for a given radiation and geometry and is independent of the phase diffracting, the bracket is

combined into a constant Q.

$$E_{\alpha(hkl)} = QA\left[e^{-2M}p \left|F_{\alpha(hkl)}\right|^2 (L.P.) \frac{1}{v_\alpha^2}\right] V_\alpha \qquad \text{Eq. (2)}$$

In Equation (2) the bracket is a constant characteristic of the diffraction line of the phase α, determined only by the composition and structure of the phase α. This constant we shall call $R_{\alpha(hkl)}$. Since A = 1 for the conditions used, (See Appendix II)

$$E_{\alpha(hkl)} = QR_{\alpha(hkl)} V_\alpha \qquad \text{Eq. (3)}$$

For a given pair of lines, say γ (220) and α (200) the ratio of the integrated intensities,

$$\frac{E_{\alpha(200)}}{E_{\gamma(220)}} = \frac{Q\ R_{\alpha(200)}\ V_\alpha}{Q\ R_{\gamma(220)}\ V_\gamma} \qquad \text{Eq. (4)}$$

and

$$\frac{V_\alpha}{V_\gamma} = \frac{E_{\alpha(200)}}{E_{\gamma(220)}} \cdot \left(\frac{R_{\gamma(220)}}{R_{\alpha(200)}}\right) \qquad \text{Eq. (5)}$$

Since $V_\alpha + V_\gamma = 100\%$ when no phases other than α and γ are present

$$\frac{V_\alpha}{V_\gamma} V_\gamma + V_\gamma = 100\%$$

$$V_\gamma \left(1 + \frac{V_\alpha}{V_\gamma}\right) = 100\%$$

$$V_\gamma = \frac{100}{1 + Z} \qquad \text{Eq.(6)}$$

where V_γ is now percent austenite by volume and $Z = \frac{V_\alpha}{V_\gamma}$

The temperature factor e^{-2M} depends on the characteristic temperature of the diffracting phase. It expresses the decrease in line intensity which is due to the fact that the atoms are not fixed, but vibrate about their mean position. Since the position of a given atom is thus not uniquely determined at every instant, a diffuse maximum occurs in the general region of the sharp reflection, the energy in the diffuse reflection being lost by the sharp line. To quote from James[8] "Temperature diffuse scattering

shows weak maxima in the same position as interference maxima, but far more diffuse. Interference maxima are reduced by e^{-2M} (The Debye Waller temperature factor)." Since the diffuse maximum due to temperature diffuse scattering appears in the same region as each sharp line, when the integrated intensities of such relatively broad lines as are found in quenched and tempered steels are measured, much of the temperature diffuse scattering is included in the "tails" of the lines. Thus we shall be closest to the truth if we apply no temperature correction factor to the intensity factors. Since the final answer is affected only by the ratio of the temperature factors for the pair of lines used, the magnitude of the correction, even if it were included, would be small for lines of not widely different 2θ values. The ratio of temperature correction factors for the γ (220) α (200) combination is about 0.98 at room temperature assuming the characteristic temperature of pure iron for both phases. Even if the temperature correction were to be applied, the question of the true characteristic temperatures of martensite and austenite cannot be answered with

certainty. It seems unlikely that they would be the same as that of pure iron. For the reasons cited, the temperature factor was called unity in these calculations.

The values of R for the lines of interest are tabulated in Appendix I, with the data required for their calculation.

The only pair of lines which should be used in patterns obtained with chromium radiation are the γ(220) and the α(200). These lines are the most widely separated ones and are subject to the least interference from adjacent lines. Figure 1a shows the proportion of cementite line intensities to those of the ferrite lines in spheroidized specimens of steel A. Figure 1b shows a pattern for Sample A-8 q which contains about 5 percent of undissolved cementite. The positions of the corresponding strong cementite lines are indicated in both patterns. Note how the γ(220) and α(200) lines fit between the lines of the cementite when it is present in the structure. This is the only pair of γ and α lines which is free from interferences of other lines in the pattern. In

a

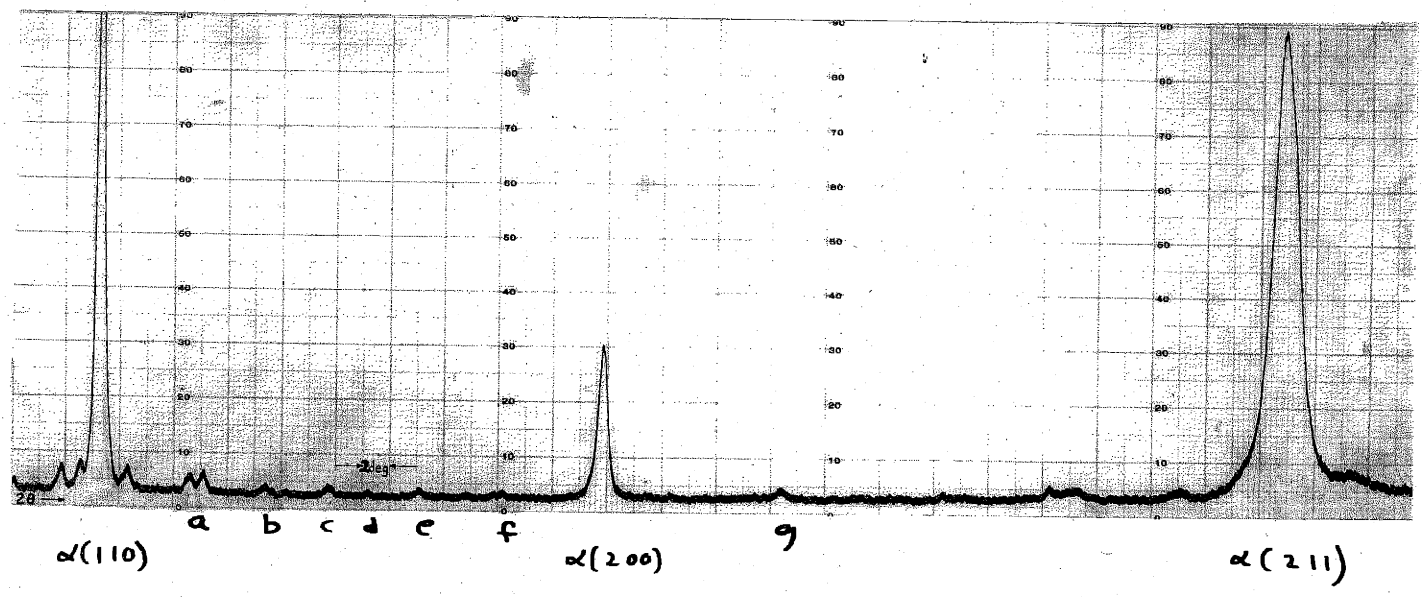

b

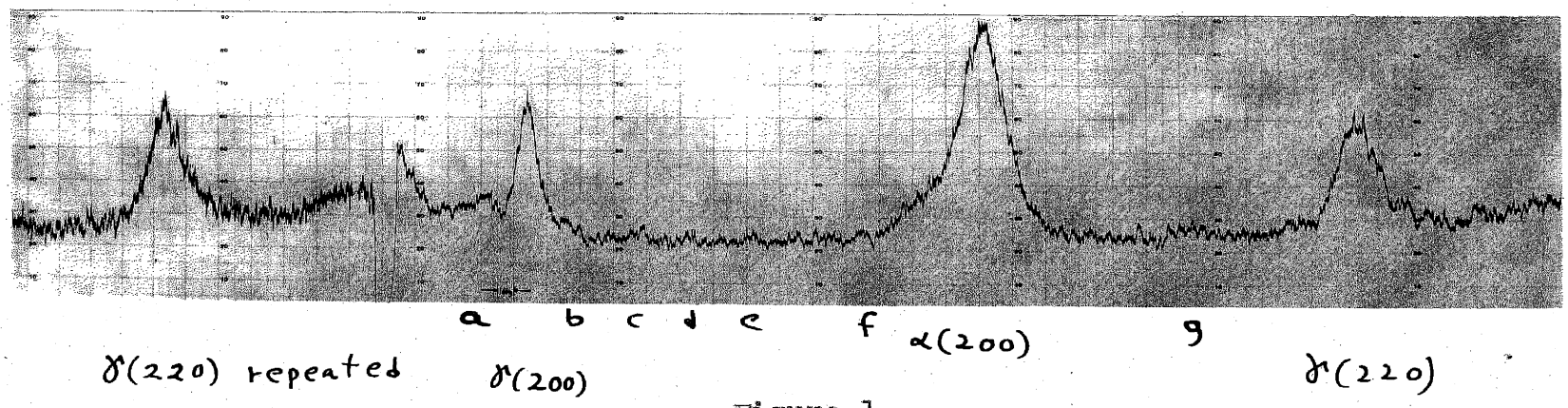

Figure 1

Recorded Patterns Showing Cementite Lines

(a) Spheroidized Steel A (b) Sample A-8 q

tempered structures none of the epsilon carbide lines[9] interfere with this pair of lines. Since engineering applications of steel A often specify heat treatments similar to that given Sample A-8 q in which undissolved carbide is retained for wear resistance, the lack of interference by the cementite lines constitutes an important reason for using the $\gamma(220)$ $\alpha(200)$ line pair for retained austenite determinations.

For all patterns made with chromium radiation, the R values were calculated considering the structure of γ and α to be made up of iron atoms only. The lattice constants used were measured from the patterns wherever possible using a silicon standard to correct observed values of 2θ. Where the tetragonality was not easily measured, the values of a_o and c_o for the martensite were taken from the extrapolation of the average data of Hagg and others.[10] The magnitudes of the corrections when the scattering factors were changed by consideration of the substitutional solution of chromium and interstitial presence of carbon are shown to be small in Appendix I.

III EXPERIMENTAL WORK

A. Materials and Equipment

The material used for most of the investigation was S.A.E. 52100, a steel in which retained austenite is the subject of great engineering interest. A sample of 1045 was also used to test the sensitivity of the method to small quantities of retained austenite. The designation and heat analysis of the steels used are listed in Table I. Steel A was received in the spheroidized condition as 5/8 inch square bar. At least 1/16 inch was removed from all sides before specimens were made to eliminate the effect of any decarburized region near the surface of the bar. The specimen of 1045 was machined from the center of a one inch round of hot rolled bar. The designations, and heat treatments of all specimens used are listed in Table II. A-1 to A-5 were sealed off in evacuated Vycor tubing to prevent oxidation and concentration gradients due to decarburizing. After the treatments indicated all of the specimens remained bright, evidence of the protection.

Table I

Steel	Percent by Weight							
	C	Mn	Si	Cr	Ni	Mo	P	S
A	1.00	.35	.28	1.44	.20	.06	.016	.013
B	.47	.79	.20	----	---	---	.012	.036

Table II

Designation	ASTM Grain Size	Austenitizing Temp. °F	Austenitizing Time (min)	Protection against Decarb.	Quenching Procedure
A-1 A-2 A-3	5-6	1900	60	Evacuated Vycor tube	Tube quenched into water at 200°F; slowly cooled to room temperature
A-5	1-2	2100	60	Evacuated Vycor tube	Tube broken; specimen quenched into oil at 75°F
A-6	5-6	1900	60	Placed between 2 other pieces of steel A	Quenched into oil at 75°F, transferred to mixture of ice and water at 32°F
A-7	5-6	1900	10	None	Quenched into oil at 75°F
A-8*	9 or finer	1550	60	Austenitized in molten lead	Quenched into oil at 75°F
B-1	7-8	1520	15	Austenitized in molten lead	Quenched into water at 75°F and violently agitated

*A-8 corresponds to the hardening of commercial applications of SAE 52100.

Grain sizes were determined from metallographic examination of quenched specimens etched with 5% Nital + Zephiran Chloride. The grain sizes at 1900°F were further checked by treating identical specimens for various times at 1900°F, and cooling under conditions which developed a cementite network in the grain boundaries. The results obtained by both methods were in agreement.

The reason for the slow cooling rate used and the choice of the temperature of the water quench used for this tube especially was to produce a condition of maximum stability against transformation at room temperatures in the retained austenite. Complete data on austenite stabilization for a 52100 type steel was available[11] and the heat treatment was planned using that data. Specimens A-1, A-2, and A-3 were sealed off in a single Vycor tube, so that they received identical treatment.

All specimens had a minimum width of 11 millimeters since the width of the area irradiated was 10 millimeters. The reason for no Vycor protection for A-6 and A-7 was that they were too large to be

easily sealed off in Vycor. Enough material was ground off to make the surfaces used reasonably free from any effect of decarburization. Table III shows the treatments subsequent to quenching. Specimen designations were modified to indicate the condition of the specimens.

All specimens were polished using standard metallographic techniques. The as quenched specimens were examined for evidences of tempering in the rough grinding operation by etching the polished specimens with 5% Nital with Zephiran Chloride. Tempered regions are darkened rapidly by this etch and it affords a sensitive method for detecting tempering due to grinding of quenched specimens. After darkening for lineal analysis, the specimens were repolished on the final polishing lap so that no differences due to surface preparation would be present. All specimens except A-3 p were given a final etch with 5% Nital + Zephiran Chloride before x-ray analysis. Specimen A-3 p was alternately polished and etched as the others, but the final etch was omitted to observe whether any difference in results would be obtained. The lines

Table III

Treatment of Specimens Subsequent to Hardening

Designation	Total depth of mat'l. removed by grinding and polishing in inches	Tempering Treatment
A-1 q	.013	none
A-1 d	.013	10 sec., 600°F
A-2 q	.008	none
A-3 q	.018	none
A-3 d	.018	10 sec., 620°F
A-3 p	.018	10 sec., 620°F
A-5 q	.010	none
A-5 d	.010	10 sec., 600°F
A-6 q	.040	none
A-7 q	.040	none
A-8 q	.005	none
B-1 q	.030	none

were broadened slightly but the results were not significantly altered. The etched specimen showed 38.3 percent austenite while A-3 p run under identical conditions showed 38.7 percent.

The major portion of the x-ray work was done with a Phillips High Angle Goniometer Recording Spectrometer. The instrument makes use of a Geiger tube operated under conditions giving a linear response to x-ray intensity over the range of intensities used. Figure 2 shows schematically the relation of x-ray source, specimen and Geiger counter tube and indicates how focussing conditions are maintained in the spectrometer. This equipment permits the recording of diffracted intensity at any value of Bragg angle θ continuously as the desired range of θ is scanned at a uniform speed synchronized with the speed of the recording chart. The specimen rotates with half the angular speed of the Geiger tube, thus maintaining focussing conditions. The advantages of focussing are good resolution and a high intensity of diffracted radiation at the focus. The chart speed is constant

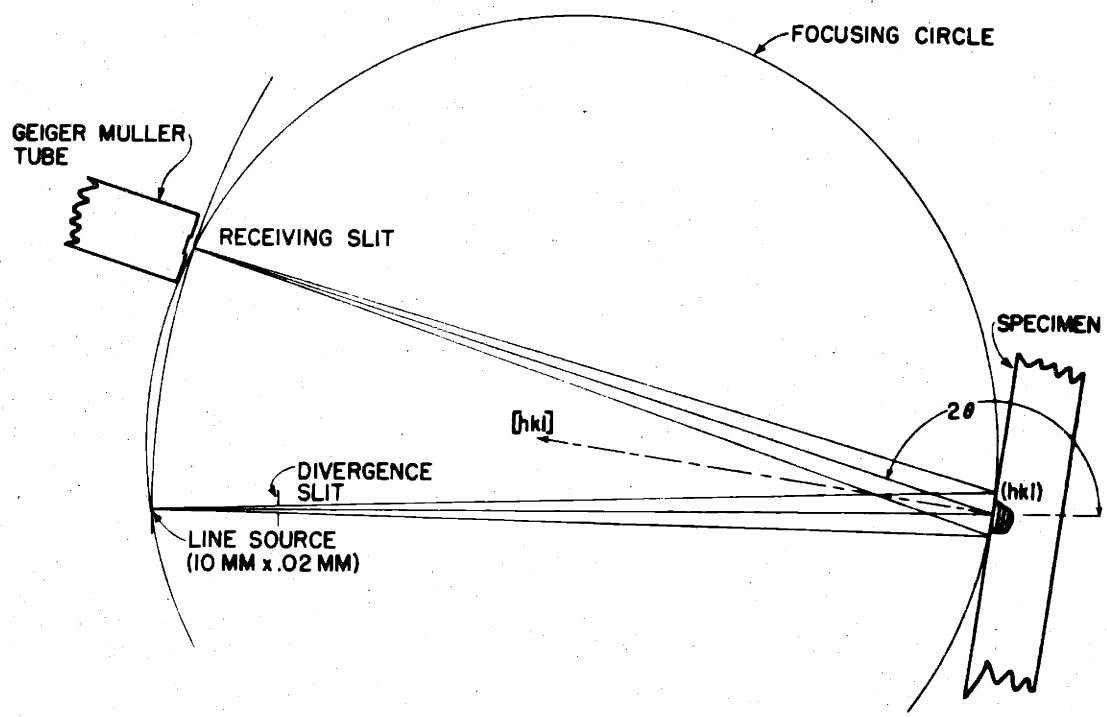

Figure 2

Arrangement of the Elements of the X-ray Spectrometer Showing Focusing Conditions

while the speed of scanning* may be varied from 1/8 degree (2θ) per minute to 2 degrees (2θ) per minute. Adjustments in the time constant of the recording circuit permits the recording pen to follow rapidly changing intensities in the region of a diffraction line. This manner of recording intensities is called a "Recorded Pattern" in this paper.

The integrated intensity (line + background) between any limits of scanning may also be measured by feeding the output of the Geiger tube to a mechanical counter and noting the reading at the beginning and end of scanning. This operation is referred to as "automatic integration". Another method of obtaining the x-ray intensities consists of setting the spectrometer at a given value of 2θ and observing the intensity as the number of counts in a given time interval are indicated by the same mechanical counter used for automatic integration.

---

* Scanning speeds are given as degrees, 2θ, per minute and refer to the travel of the Geiger tube.

This technique is called "Point Counting". It is most often done by measuring the time for a fixed number of counts, thus giving a constant probable error in all intensities so measured.

B. Radiation and Filtering

Chromium, iron and cobalt radiations were tried, but only chromium was found useful over a wide range of austenite contents. With the equipment used, it was not possible to use crystal-monochromated radiation. Monochromation of the beam had to be achieved through the use of appropriate filters. For most work on a spectrometer, it is sufficient to reduce the K_β intensity to a negligible level through the use of a filter containing the element having its K absorption edge between the $K\alpha$ and K_β wave lengths of the radiation being used. The normal position for such a filter is between the diffracting specimen and the Geiger tube where it is also effective in filtering out much of the fluorescence of the specimen by the K_β and "white" components of the target spectrum.

When chromium radiation was used on a specimen consisting almost entirely of iron, the use of vanadium, the standard K_β filter for chromium radiation, achieved a continually increasing contrast between the characteristic radiation and the background as the thickness of the filter was increased up to a limit. The reason for increasing contrast with filter thickness is that the mass absorption coefficient of vanadium for the wavelength of chromium K_α radiation is 77.3 as compared to 422 for iron K_α. The iron fluorescence is probably the strongest component of the high background observed when only enough vanadium is used to suppress the K_β of the chromium radiation. With iron radiation and an iron specimen the condition relative to fluorescence is at its worst, since the radiation being diffracted is of the same wavelength as the component of the background which must be filtered out. The situation with cobalt radiation is only slightly better than with iron. An iron filter was employed between source and specimen to remove the K_β and some of the white radiation, thus minimizing iron

fluorescence. A comparison of recorded patterns made under optimum conditions with each radiation on the same specimen is shown in Figure 3. With chromium radiation filtered with vanadium, the line energies could be measured with the least interference of background.

Another method of improving contrast of diffracted lines to background was found. By lowering the voltage between the filament and target in the x-ray tube, two important effects are obtained; the shortest wavelength in the spectrum is longer, and the total energy in the "white radiation hump" of the tube spectrum is reduced. Both of these effects decrease the energy expended as fluorescence and the background is again reduced more rapidly than the chromium K_{α}. The combined effect of these two methods of improving contrast is shown in Figure 4. The peak to background ratio was obtained in each case by point counting the intensity at the peak of the (220) austenite line and at a given value of 2θ in the background away from the line; the counts being taken at the same pair of 2θ settings for each

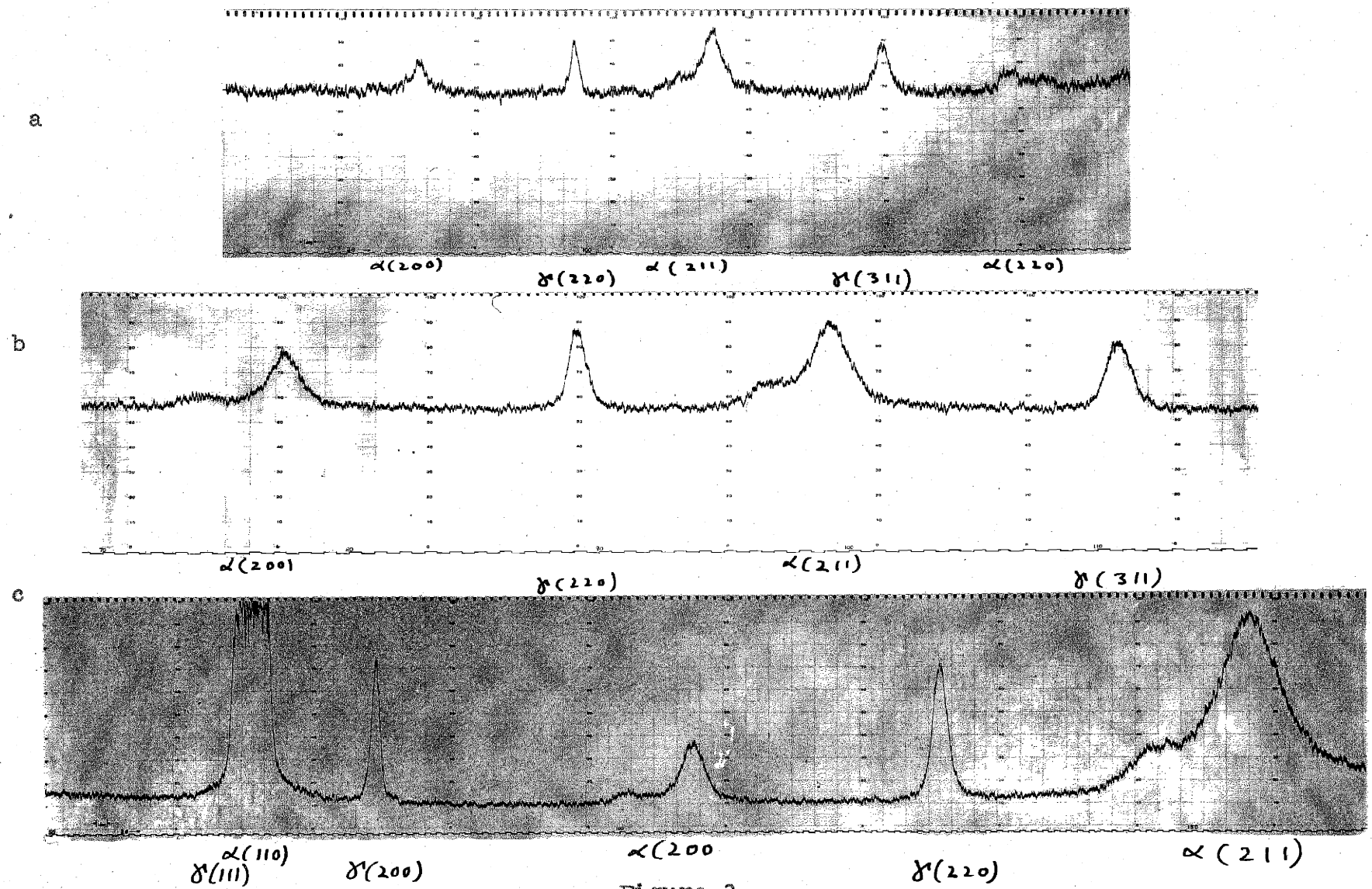

Figure 3

Comparison of Patterns of Sample A-6 q Made Using
(a) Iron Radiation Filtered with Manganese Oxide (b) Cobalt Radiation Filtered with Iron Foil
(c) Chromium Radiation Filtered with Vanadium Foil

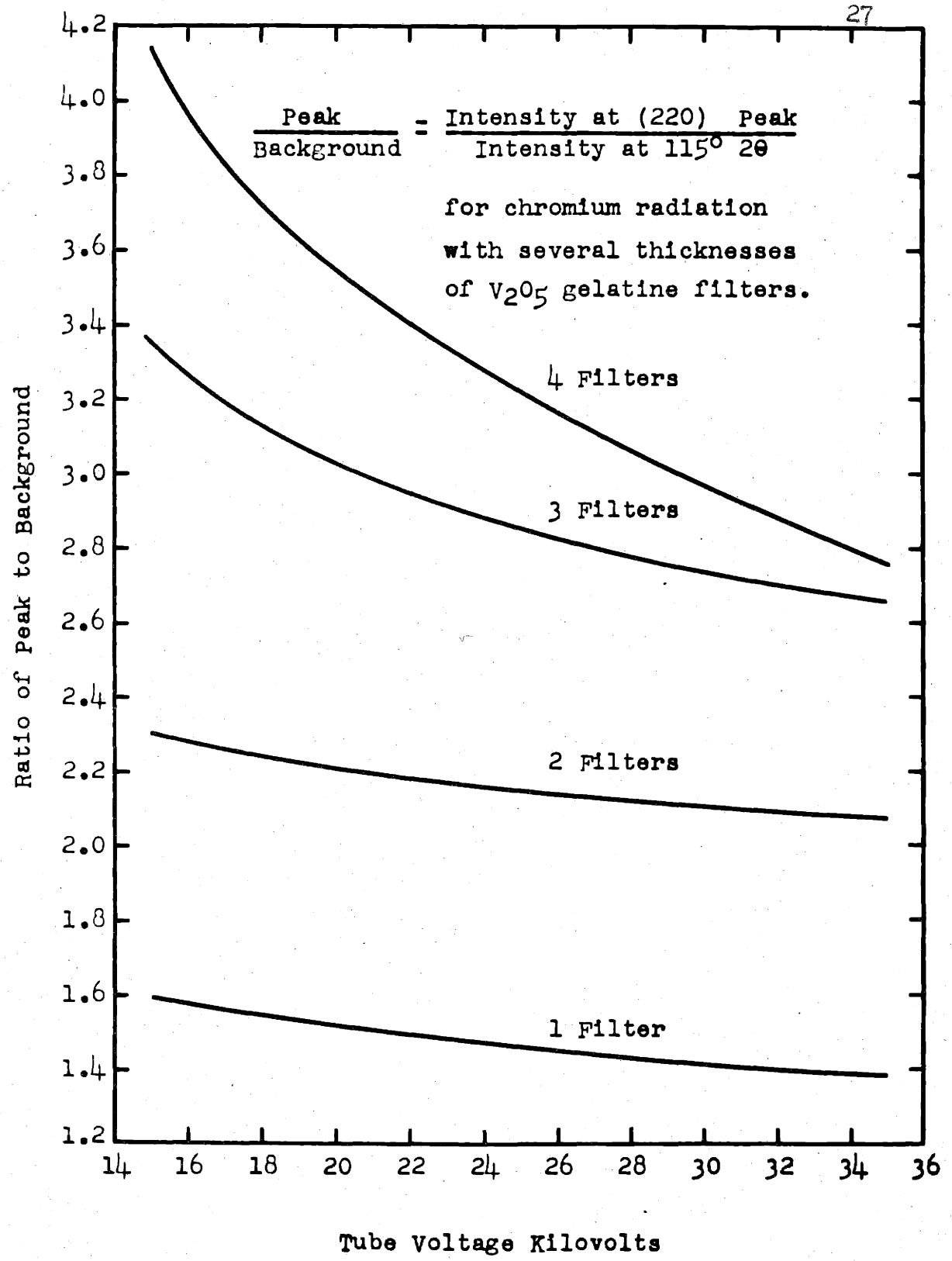

Figure 4

Effect of Filtering and Tube Voltage on Contrast

point in the plot. The power input to the tube was maintained constant by increasing the tube current as the tube voltage was lowered.

Both methods of producing better contrast were obtained at the expense of a decrease in the intensity level of the pattern. For patterns recorded continuously or automatically integrated the effect of a lowered intensity level was to increase the influence of statistical fluctuations in x-ray intensity on the smoothness of the pattern. A higher time constant tended to minimize this in a recorded pattern, but with a high time constant, lower scanning speeds had to be employed to prevent shifting and mechanical distortion of the line shapes which would invalidate any quantitative comparison of integrated line energies. For the automatically integrated pattern, the effect was to decrease the reproducibility of results for a given scanning speed. For point counting, the effect was to increase the time required to maintain the same probable error, and the effect on all methods of integration was that improved accuracy was gained at the expense of time.

Fortunately, a way was found to make use of the methods for enhancing contrast without increasing the time required for a reasonable degree of accuracy. Ordinarily, the slit which is placed at the focus of the spectrometer to limit the width "seen" by the Geiger tube is 0.006 inches wide when a 4 degree divergence slit is used at the x-ray tube to limit the divergence of the incident beam on the specimen. A slit of such a width is necessary for good resolution of sharp lines, but it should be noted that the diffraction lines in a hardened steel are by no means sharp. Even the austenite line widths measured at half height in the samples used in this investigation were consistently in excess of 1 degree 2θ. The use of wider slits at the focus permitted a much higher degree of filtering and lowering of tube voltage with little or no resultant line broadening. Both 0.020 and 0.060 inch slits were used, these being equivalent to 0.17 and 0.54 degrees 2θ respectively on the spectrometer used. The effect of slit width on the intensity ratios was examined and found to be negligible for the slits used.

The vanadium for filtering was used first in the form of vanadium oxide in gelatine sheets as is common practice. X-ray work being done elsewhere[12] with chromium radiation had emphasized the benefits to be gained by the use of metallic vanadium in the form of foil of suitable thickness rather than the oxide. A small quantity of vanadium was obtained in the form of foil in two thicknesses, 0.0012 and 0.0025 inches. Although the thickness in each sheet was not perfectly uniform, it was possible to find areas large enough to permit cutting out of filters in which the thickness was very uniform. Experiments showed a striking increase in filtering efficiency as shown by the data in Table IV. The same sample, tube voltage, current, and slit combination was used for all of the patterns from which the data comprising Table IV was taken. The only variable was the filter used. In addition to the marked improvement on replacing the oxide filters with metallic foil, it was found that once the iron fluorescence was reduced to the point where it was no longer the major component of the background, further filtering with vanadium was harmful rather than beneficial as indicated by the decrease in peak to background ratio in going from the thin to the heavy

Table IV

Effect of Filtering on Contrast between a Diffraction Line and Background

Pattern Number	$\frac{\gamma(220) \text{ Peak Intensity}}{\text{Background @ } 115^\circ\ 2\theta}$	Filtering
PCP-10	$\frac{128 \text{ cps}}{43 \text{ cps}} = 3.0$	$3V_2O_5$(gelatine filters)
AIP-3	$\frac{175 \text{ cps}}{36.5 \text{ cps}} = 8.33$	.0012 inch vanadium foil
AIP-6	$\frac{194 \text{ cps}}{23.4 \text{ cps}} = 8.30$	.0012 inch vanadium foil
AIP-2	$\frac{55.6 \text{ cps}}{7.65 \text{ cps}} = 7.27$	.0025 inch vanadium foil

All intensities are in counts per second; all patterns made using the short chromium tube operated at 25 KV 15 ma, .060 inch slit. Specimen A-2 q used in all cases.

vanadium foil. Other data substantiated the existence of a maximum in contrast at some intermediate filter thickness. If a number of very thin foils had been available, curves similar to those of Figure 4 might have been determined for increasing numbers of vanadium metal filters and the optimum thickness of metallic filter determined. The general shape and relation of the curves might be somewhat different from those of Figure 4 but the tendency toward an optimum filter thickness for a given tube voltage is indicated even in Figure 4. The intensity level present with the 0.0012 inch foil is on the low side of what appears to be the practical working range for rapid determinations of retained austenite with a good degree of accuracy. The optimum metallic vanadium filter thickness for the conditions used was estimated to be 0.001 inch. The optimum operating conditions consistent with a good tube life expectation were found to be 25 killovolts and 15 milliamperes for the chromium tube.

C. Effect of Grain Size and Preferred Orientation

The equations relating line intensities are applicable only to patterns in which the Debye Scherrer cones are composed of a sufficient number of diffracted beams from individual grains to produce continuous lines of uniform intensity per unit length. This condition is not met if any degree of preferred orientation exists in the sample. The steels used were checked for preferred orientation by taking front reflection x-ray patterns using cobalt radiation. The arrangement of tube, specimen and film is shown schematically in Figure 5. Figure 6a shows a reproduction of the film obtained for the spheroidized (as received) 52100 steel. Since no preferred orientation was found in the annealed material, no preferred orientation should exist in the hardened steel, but the film of Figure 6b was made to insure that no preferred orientation was present in Sample A-8 q.

Figure 6c showed no preferred orientation in Sample A-6 q but illustrates the effect of coarse grain size.

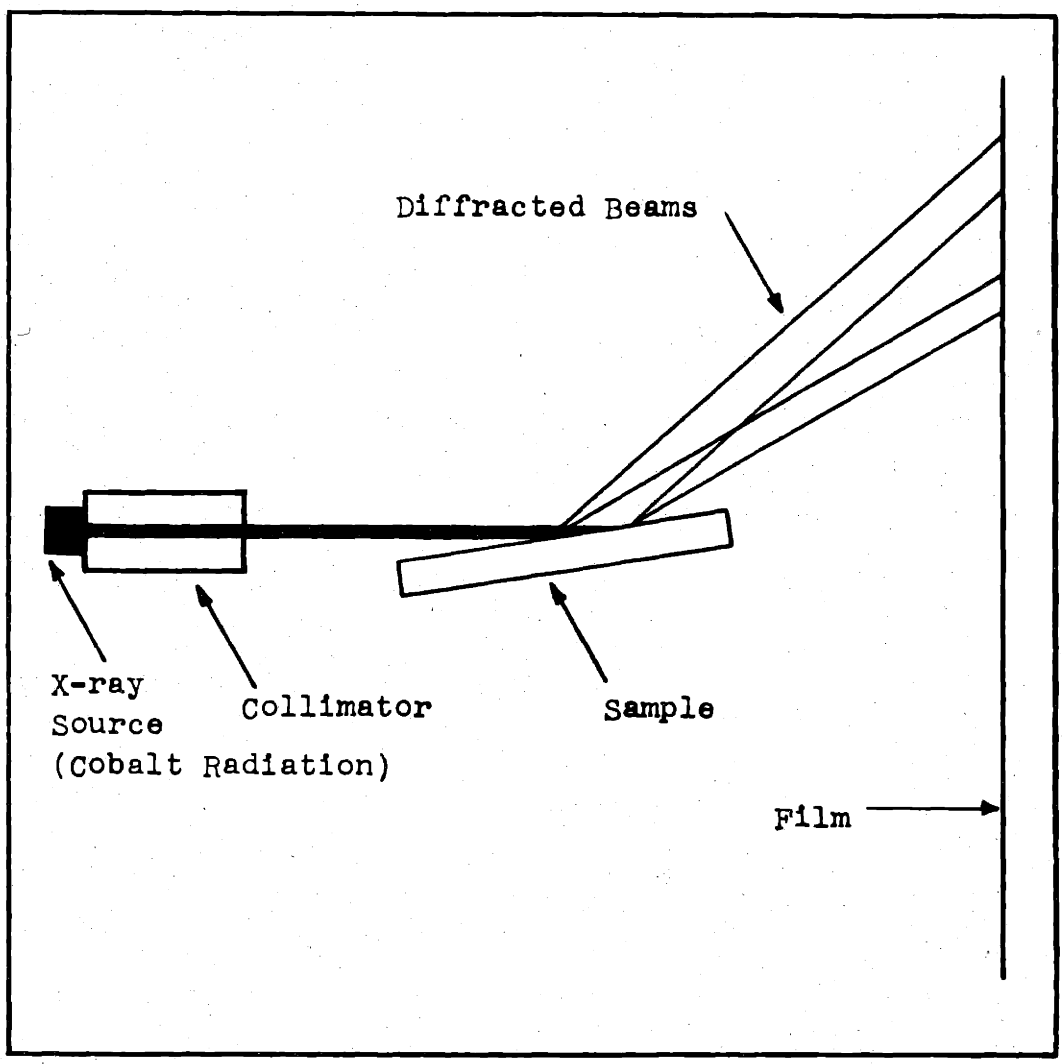

Figure 5

Arrangement of X-ray Source, Sample, and Film for Front Reflection Films.

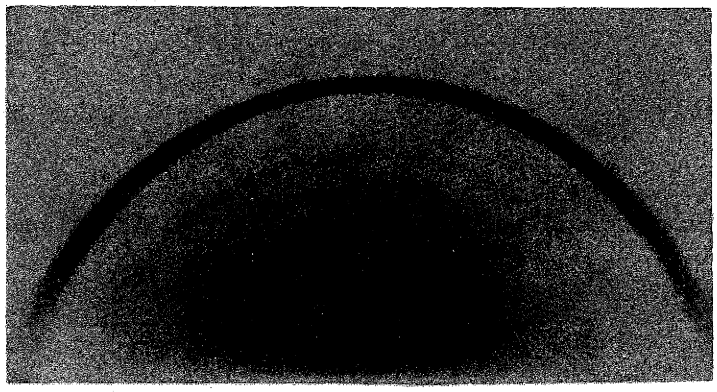

a. Spheroidized Steel A. Outside ring is α(110), inside rings are strong cementite lines.

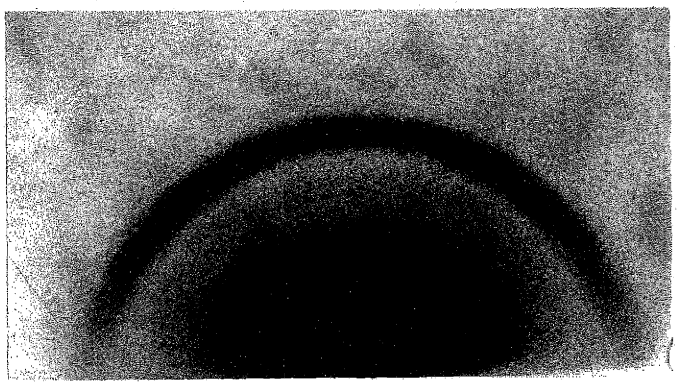

b. Sample A-8 q. Ring consists of α(110) and γ(111).

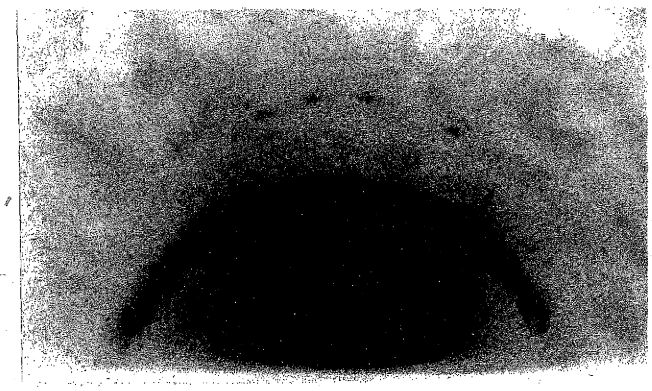

c. Sample A-6 q. Inner ring consists α(110) and γ(111). Outer ring is γ(200).

Figure 6
Front Reflection Patterns Recorded on Films Using Unfiltered Cobalt Radiation

When the grain size of a polycrystalline sample becomes too large, the diffraction lines become spotty and are no longer of uniform intensity. When such a grain size is present the sample is usually rotated to give continuous lines. The specimens used in the photographic method(1) were rotated when the grain size exceeded A.S.T.M. 7. Since it was not possible to rotate the specimen on the spectrometer, the diffraction lines were checked to determine whether they were continuous. A film was wrapped in aluminum foil and placed as near as possible to the focus of the spectrometer, the instrument being set at the reflection peak being checked. Figures 7a and 7b show that the Specimen A-6 q does give a continuous line on the spectrometer with chromium or cobalt radiation where a much larger area is irradiated than in the front reflection picture. The diffracting volume on the spectrometer using the four degree divergence slit at the x-ray tube is about one hundred times that in the front reflection arrangement. Furthermore, the multiplicity factors of the γ(220) lines shown in Figure 7 are twice that of the spotty γ(200) line

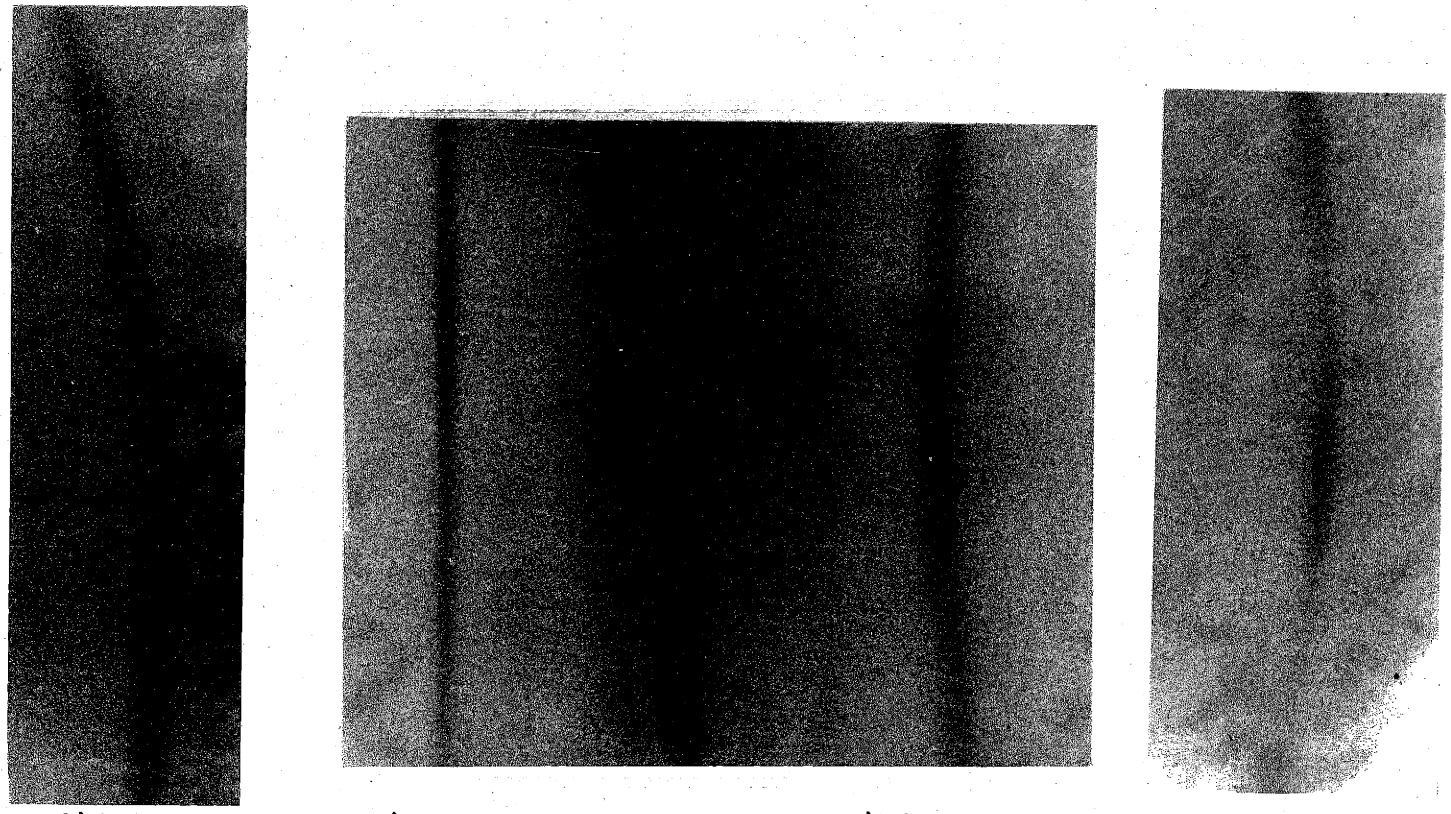

a γ(220) b γ(220) α(211) γ(311) c γ(220)

Figure 7
Diffraction Lines Recorded Photographically at Spectrometer Focus
(a) γ(220) line; Sample A-6 q; Chromium Radiation
(b) γ(220) line; Sample A-6 q in Focus; α(211) and γ(311) out of Focus
Cobalt Radiation
(c) γ(220) line; Sample A-5 q; Chromium Radiation

shown in Figure 6c. The same sample was used for Figures 6c, 7a, and 7b. The reproductions of the front reflection films, unfortunately, do not show all of the spots visible on the original films, some of the weak austenite spots are lost in the reproduction of the films. Figure 7b shows the continuous nature of three lines in the pattern of A-6 q for cobalt radiation on the spectrometer. Sample A-6 q showed a grain size of 5 to 6 on the A.S.T.M. scale. The upper grain size limit for the spectrometer is indicated in Figure 7c by the fact that Sample A-5 q shows a γ (220) line which is not continuous for chromium radiation on the spectrometer. Since the grain size for A-5 q was found to be A.S.T.M. 1 to 2 the limit of practical use of the spectrometer technique without sample rotation must be between these grain sizes, the best estimate being A.S.T.M. 4.

D. Operation and Integration

A large number of patterns were run using all three methods of obtaining the x-ray intensities as a function of 2θ. When the intensities were recorded

on the chart automatically, the scale factor was adjusted to keep the peak of the strongest line being measured just inside the chart boundaries. The time constant was adjusted according to the speed of scanning and line sharpness so that the true shape of the lines was recorded. A smooth curve was drawn through the recorded line and connecting the background levels between the diffraction lines. The area included under a given diffraction line above the background was directly proportional to the total line energy, designated as $E_{(hkl)}$ in the calculations. Since the line energies entered into the calculations as ratios, no conversions were necessary so long as the lines were recorded under identical conditions and measured in the same units.

When the lines were automatically integrated, it was necessary first to record the pattern at high speed, picking the limits for automatic integration from this chart. The scheme for determining the background when using automatic integration is shown diagrammatically in Figure 8 using the average data

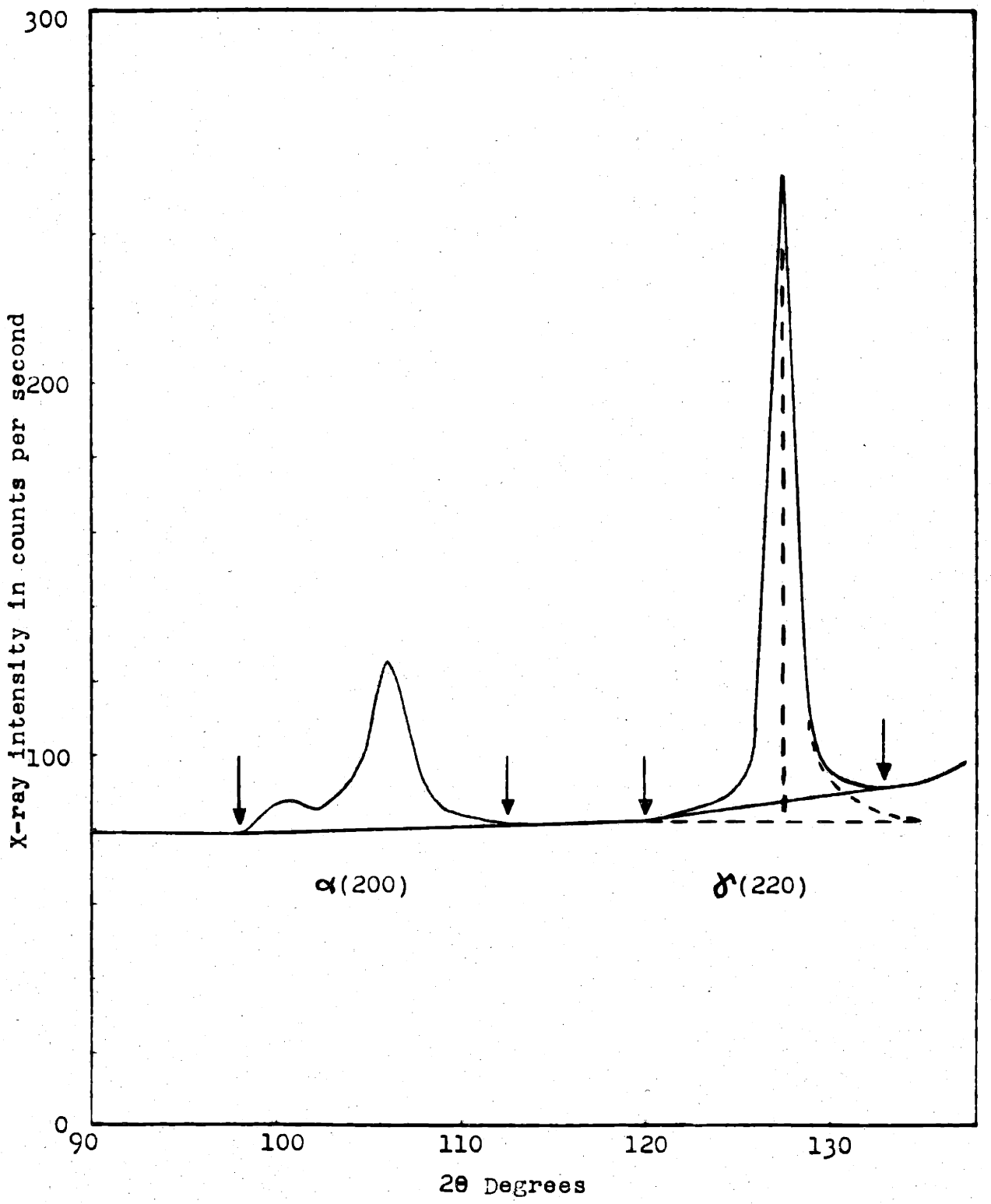

Figure 8

Methods 1 and 2 for Automatic Integration
Illustrated Schematically

of Point Count Patterns 4, 5, and 6 for the plot of intensity against 2θ.

Method 1, indicated by the broken lines, was based on the premise that the background could be considered flat and that the γ (220) line was symmetrical. The entire α (200) line was scanned between the limits indicated by the arrows. The α (200) background was determined by recording the total number of counts with the spectrometer set at the low angle end of the α(200) line for the same time required to scan the whole line. The γ (220) line was scanned from the arrow at the low angle side of the center of the peak. This integrated intensity was doubled to give ($E_{\gamma(220)}$ background). The background count was obtained for the γ (220) line by recording the total number of counts when the spectrometer was set to the low angle limit of the γ (220) line for a time corresponding to the scanning of the whole line.

The precision with which the line center had to be located was well within obtainable limits. In A.I.P. 4, the scanning was purposely ended away

from the line center. One count was run 0.04 degrees past the center and another stopped 0.06 short of the line center. The results are shown in Table V. The errors involved were within the reporducibility of repeated counts to the true center.

Table V

Effect of Erroneous Location of the Line Center on Results by Automatic Integration Using Method 1

(data from A.I.P. 4)

Degrees 2θ Scanned (½ of (220) line)	Error in end of Scanning degrees 2θ	% γ
117.7 - 127.7	- 0.06	38.2
117.8 - 127.8	— 0.04	40.3
117.76-127.76	0	40.2

Method 1 was tried because it was felt that possibly the sharp increase in the rate of background rise on the high angle side of the γ(220) line might be due to interaction between the high angle extremity

of that line with the huge α(211) line as is indicated in Figure 9. The behavior of the background beyond 165 degrees 2θ could not be examined since that is the upper limit of travel for the goniometer. Even observing the background beyond the sharp α(211) line for the spheroidized specimen yielded little information, because the intensity still had not reached a definite minimum at 165° 2θ.

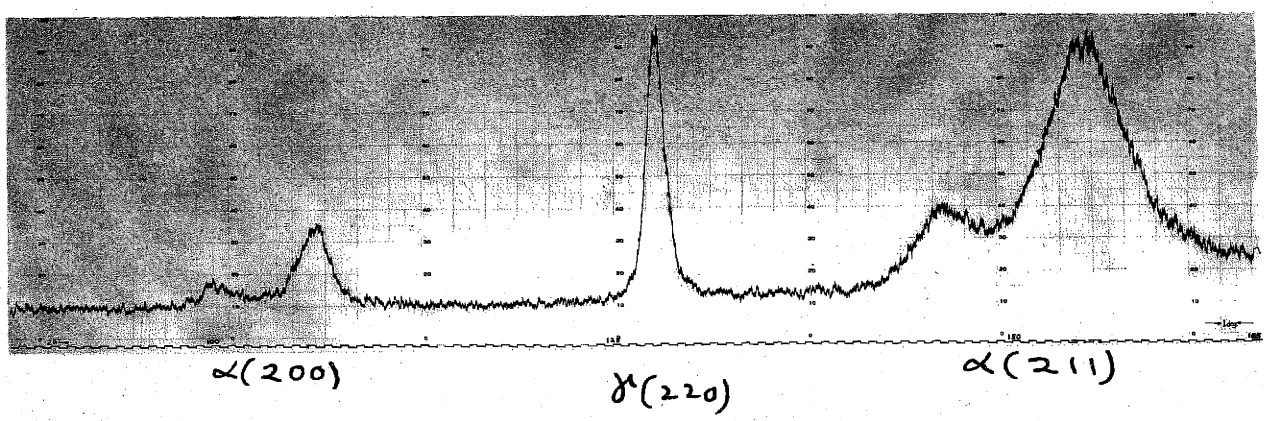

Figure 9

Recorded Pattern of Sample A-7 q Showing Possible Interaction between γ(220) and α(211)

To the end that the true background behavior might be appraised, specimens (A-6 and A-7) much longer than those used previously, were heat-treated and prepared to permit examination of the background at the

low angle extremity of the region of interest, still maintaining the condition that the irradiated area never exceeded the specimen boundaries (See Appendix II). The patterns made using the long specimens gave information on the general background trend as is shown in Figure 3c and Figure 10 which indicates a general shape having a flat minimum and rising at both ends. The background trend has been sketched in for Figure 10. After these patterns had been obtained, all automatically integrated patterns were made and calculated by Method 2, indicated by solid lines in Figure 8. This method assumed a linear background for the region under the line and the scanning included the whole line. Background for each line was taken as the mean of the background intensities at both extremities of the line indicated by the arrows. This represented the best compromise of the true background shape with the limitations of the automatic integration method.

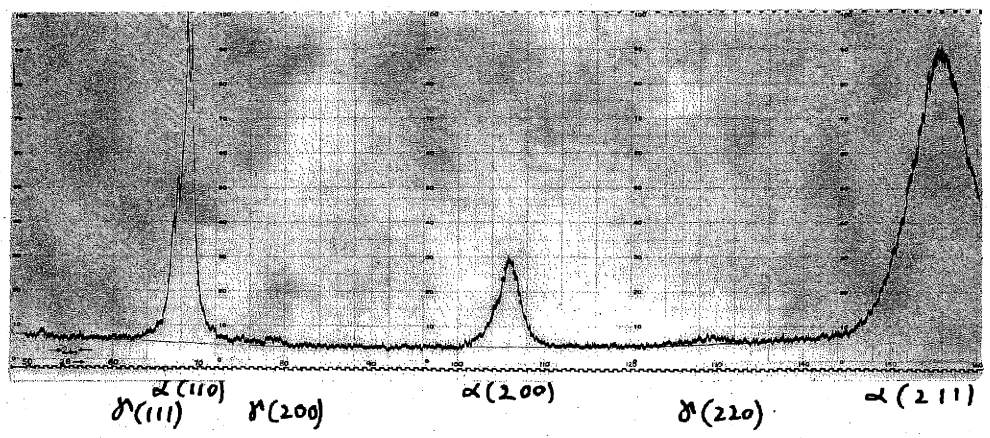

Figure 10

Recorded Pattern of Sample B-1 q Illustrating the Background Trend

An evaluation of the expected effect of using Method 1 as compared to Method 2 was made by performing geometrically the same integrations made automatically. This was done using the averages of the point counts from P.C.P. 4, 5, and 6. The results of this comparison are shown in Table VI. Examination of the background shape would lead one to expect exactly what is observed. Method 1 gives consistently higher results, a fact borne out by a comparison of Method 1 Automatically Integrated Patterns with the results obtained by other methods on the same specimens.

Table VI

Comparison of Method 1 and Method 2

	Limits of Integration for γ (220) line $^{\circ}2\theta$	% γ
Method 1	120 - line center	42.0
	115 - line center	43.6
Method 2	120 - 133	39.6
	115 - 135	37.5

Plot of the average data of P.C.P. 4, 5, and 6 as shown in Figure 8 was integrated graphically as indicated above.

The point counted patterns were simply plotted, the best curves drawn for lines and background, and the line energies taken as the area included by the line above the background as measured by a planimeter. Areas integrated by planimeter could be reproduced within 1 percent for repeated measurement of the same area. When the planimeter was used for line integration (on recorded patterns and point count patterns after plotting) the value recorded for the line was the average of three measurements of that

line. One line area recorded by the planimeter was checked against algebraic integration of the same area using Simpson's Rule. The difference was less than 1 percent.

Two of the specimens used in the investigation were tempered at 600 - 620°F to darken the martensite present while leaving the austenite substantially unaffected. The retained austenite in the specimens was determined by lineal analysis. The results are shown in Table VII.

E. Results

The data indicates that the optimum conditions for the operation of a chromium tube under 400 watts is to use a combination of 25 KV and 15 - 16 ma filtered with vanadium foil about 0.001 inches thick. These conditions yield a maximum contrast between diffraction lines and the background.

A complete listing of the results obtained from all types of patterns is given in Table VIII with pertinent operating information.

Table VII

Comparison of Percent Austenite from Lineal Analysis with X-ray Results

Specimen	X-ray Results, Pure Iron Scattering Results from Table VIII				Lineal Analysis "d"
	Pattern	"q"	Pattern	"d"	
A-3	R.P. 1	34.0	R.P. 4	37.6	38.6
	R.P. 2	36.6	R.P. 5	37.5	39.7
	R.P. 3	37.2	R.P. 6	37.3	37.1
	P.C.P. 1	38.8	A.I.P. 4	40.2	36.7
	P.C.P. 3	37.8	A.I.P. 5	40.0	
	P.C.P. 4	38.2	P.C.P. 8	38.3	
	P.C.P. 5	39.1			
	P.C.P. 6	39.1			
	P.C.P. 7	39.2			
A-1	A.I.P. 8	36.0			31.3
					33.5

Table VIII

Tabulation of Results

Pattern Number	% γ, Iron Scattering Only	Filter	Tube KV	Tube ma	Recording Conditions SF	Recording Conditions M	Recording Conditions TS	Scanning Speed	Width of Slit at Focus, in.	$\frac{E_{\alpha(200)}}{E_{\gamma(220)}}$
					Sample A-3 q (Chromium Radiation)					
R.P. 1	34.0	g	16	10	2	.6	16	1/2	.060	.7604
R.P. 2	36.6	g	20	17.5	4	1	4	1/2	.060	.678
R.P. 3	37.2	g	30	12	8	.8	8	1/2	.060	.6617
P.C.P. 1	38.8	g	20	10	32				.060	.6177
P.C.P. 3	37.8	g	20	10	32				.060	.6455
P.C.P. 4	38.2	g	30	12	32				.060	.6338
P.C.P. 5	39.1	g	30	12	32				.060	.6119
P.C.P. 6	39.1	g	30	12	32				.060	.6104
P.C.P. 7	39.2	g	30	12	64				.060	.609
					Sample A-3 d (Chromium Radiation)					
R.P. 4	37.6	g	30	12	4	1	8	1/2	.060	.6521
R.P. 5	37.5	g	30	12	4	1	8	1/2	.060	.6537
R.P. 6	37.3	g	20	18	4	.8	8	1/2	.060	.6592

Table VIII
continued

Pattern Number	% γ Iron Scattering Only	Filter	Tube KV	Tube ma	Recording Conditions SF	Recording Conditions M	Recording Conditions TC	Scanning Speed	Width of Slit at Focus, in.	$\frac{E_{\alpha(200)}}{E_{\gamma(220)}}$
Sample A-3 d (Chromium Radiation)										
A.I.P. 4(1)	40.2	f_2	25	15	32			2	.060	.585
A.I.P. 5(1)	40.0	f_2	25	15	32			2	.060	.588
P.C.P. 8*	38.3	f_3	35	22	1% P.E.					.6323
(Sample A-1 q (Chromium Radiation)										
A.I.P. 8(1)	36.0	f_1	25	15	64			2	.060	.698
Sample A-2 q (Chromium Radiation)										
A.I.P. 1(1)	37.3	g	25	15	32			2	.060	.659
A.I.P. 3(1)	39.2	f_1	25	15	32			2	.060	.609
A.I.P. 6(1)	39.0	f_1	25	15	32			2	.060	.613
A.I.P. 2(1)	43.4	f_2	25	15	16			2	.060	.511
P.C.P.10	35.8	g	25	15	32				.060	.702
Sample A-3 p (Chromium Radiation)										
P.C.P. 9*	38.7	f_3	35	22	1% P.E.					.6221

Table VIII
continued

Pattern Number	% γ Iron Scattering Only	Filter	Tube KV	Tube ma	Recording Conditions SF	Recording Conditions M	Recording Conditions TC	Scanning Speed	Width of Slit at Focus, in.	$\frac{E_{\alpha(200)}}{E_{\gamma(220)}}$
				Sample A-6 q (Chromium Radiation)						
R. P. 20	28.5	f_2	25	15	4	1	4	1/2	.060	.982
R. P. 21	29.6	f_2	25	15	4	1	4	1/2	.060	.931
R.P. 33	29.6	f_2	25	15	8	.6	4	1	.060	.9318
				Sample A-6 q (Cobalt Radiation)						
R.P. 24	30.0	f_4	25	20	16	.8	4	1/2	.060	1.60
				Sample A-7 q (Chromium Radiation)						
R.P. 27	36.5	f_2	25	15	4	1	4	1	.060	.683
R.P. 28	36.8	f_2	25	15	4	1	4	1	.060	.672
R.P. 37	33.3	f_2	25	15	2	.8	4	1	.020	.784
R.P. 38	34.2	f_2	25	15	8	.6	4	1	.060	.755
A.I.P. 11(2)	40.0	f_2	25	15	32			1	.060	.587

Table VIII
Continued

Pattern Number	% γ, Iron Scattering Only	Filter	Tube KV	Tube ma	Recording Conditions SF	Recording Conditions M	Recording Conditions TC	Scanning Speed	Width of Slit at Focus, in.	$\frac{E_{\alpha(200)}}{E_{\gamma(220)}}$
			Sample A-8 q (Chromium Radiation)							
R.P. 23	12.2	f_2	25	15	2	1	4	1/2	.060	2.62
R.P. 34	13.3	f_2	25	15	2	.8	8	1	.060	2.37
			Sample B-1 q (Chromium Radiation)							
R.P. 25	3.2	f_2	25	15	2	1	4	1	.060	11.6
R.P. 36	2.4	f_2	25	15	4	.6	4	1	.060	15.2

g - 3 vanadium oxide filters

f_1 - 0.0012 in. vanadium foil

f_2 - 0.0025 in. vanadium foil

f_3 - approximately 0.0035 in. vanadium foil

f_4 - approximately 0.002 in. iron foil

(1) Method 1

(2) Method 2

* Point Count Pattern 8 and 9 were run on a General Electric X-Ray Spectrometer at the Research Laboratory of the Timken Roller Bearing Co., Canton, Ohio.

For several patterns the ratio of two line energies in the pattern of the same phase was measured. If the values of $R_{(hkl)}$ are correct, the ratio of $\frac{R\,\gamma(220)}{R\,\gamma(200)}$, for instance, should be equal to $\frac{E\,\gamma(220)}{E\,\gamma(200)}$.

Table IX shows the agreement of experimentally obtained energy ratios with the calculated values. The agreement is not bad considering the interferences of other lines with $\alpha(211)$ and $\gamma(200)$. Since these ratios are obtained from lines more widely separated than the $\gamma(220)$ -- $\alpha(200)$ pair, the R values may be used with confidence.

The results of the comparison of the x-ray results for sample A-3 q, A-3 d, and A-1 q with lineal analysis are given in Table VII. The results in Table VII were all calculated for iron scattering only with $\alpha + \gamma = 100\%$. The x-ray answers for darkened specimens are therefore high since some carbide precipitated during the tempering treatment. The significant comparison in Table VII is between x-ray results for "q" specimens and the lineal analyses. The agreement is quite acceptable. Point count patterns tended to give consistently higher average percent

Table IX

Comparison of Observed and Calculated Intensity Ratios for Lines from the Same Phase

Pattern	Sample	Observed	Calculated: Iron Scattering only	Calculated: Corrected for C and Cr
			$\frac{R_{\gamma(220)}}{R_{\gamma(200)}}$	
R.P. 20	A-6 q	1.46	1.55	1.55
R.P. 21	A-6 q	1.38	1.55	1.55
R.P. 22	A-6 q	1.37	1.55	1.55
R.P. 33	A-6 q	1.42	1.55	1.55
R.P. 34	A-8 q	1.58	1.56	1.57
R.P. 25	B-1 q	1.44	1.60	1.60
			$\frac{R_{\alpha(211)}}{R_{\alpha(200)}}$	
R.P. 33	A-6 q	7.13	9.1	8.8
R.P. 27	A-7 q	7.10	9.1	8.8
R.P. 28	A-7 q	6.99	9.1	8.8

austenite than the recorded patterns for as quenched specimens (condition "q"). As expected, the automatically integrated patterns gave results somewhat higher than lineal analysis.

The effect of corrections for the scattering by chromium and carbon atoms in the lattice was calculated to be small when chromium radiation was used. The reason for the small changes in results when the corrections are made is because they affect the γ(220) and α(200) lines in the same direction, so their ratio is practically unchanged. Another effect of carbon content on the calculation of R values is to change the volume of the unit cells. Again, for as quenched samples, the α and γ cells are affected in the same direction. For tempered specimens the carbon content of the martensite is decreased while that of the austenite is unchanged. This decreases the volume of the martensite unit cell tending to increase $R_{\alpha(hkl)}$. The carbon scattering correction, however, acts in the opposite direction so that the R ratio for the γ(220) and α(200) lines is substantially unchanged as tempering

proceeds. The net effect of these corrections is negligible when chromium radiation is used as the data in Table IX indicate. The ratio of two lines of the same phase could be made only approximately because of interferences from other lines or background uncertainties.

Taking the data from Recorded Pattern 4 the effect of various corrections applied are shown in Table X. The correction for the change in volume of the unit cell in going from a 1 percent carbon austenite to 1% carbon austenite with a tempered martensite of 0.6% carbon changes the percent austenite by less than 0.3% of austenite. The most important effect of tempering on the calculation is that the precipitation of epsilon carbide during tempering takes iron atoms as well as carbon from the alpha lattice. Thus after precipitation of epsilon carbide, alpha plus gamma is no longer equal to 100%. The actual volume of epsilon carbide precipitated could be estimated for a given degree of tempering but the extent by which the alpha line intensities are reduced by the precipitation of what is probably a

a coherent carbide[9] is only the subject of conjecture. The magnitude of the change in the answer for 5 and 10 percent of any carbide present in the structure is shown in Table X.

The percent austenite obtained with cobalt radiation is shown in Table XIA which shows how the percent austenite varies when calculated from all the possible combinations of line pairs. The average results are in agreement with the patterns made using chromium radiation on the same specimen. The small scatter observed in making use of all the different line combinations is further evidence of the reliability of the R factor calculations. A comparison of R ratios is made in Table XIB which offers further support for these calculations.

With the recorded patterns made at one degree per minute a single retained austenite determination can be made in one hour. Three-fourths of this time would be spent in automatic recording of the pattern, 15 minutes being allowed for measurement of the line areas with a planimeter and the simple calculations required to convert the area ratio to the percent retained austenite.

Table X

Effect of Corrections for Tempering on the Results from Recorded Pattern 4

% Carbon		Corrections Made			$\frac{R_{\gamma(220)}}{R_{\alpha(200)}}$	% γ
Austenite	Martensite	Vol of unit cell	Carbon Scattering	$(\alpha+\gamma)$%		
1.00	1.00			100	2.55	37.6
1.00	0.60	x		100	2.51	37.9
1.00	0.60	x		95	2.51	36.0
1.00	0.25	x		95	2.46	36.5
1.00	0.25	x	x	95	2.53	35.9
1.00	0.25	x	x	90	2.53	34.0

Table XI

Results with Cobalt Radiation

A. Percent austenite from all possible line pairs

Line Pair Used		% Austenite	
α	γ	Iron and Chromium* Scattering only	Corrected for Carbon
200	220	30.0	30.1
200	311	26.0	26.6
211	220	33.4	32.7
211	311	28.5	28.9
	Averages	29.5	29.6

* The correction for chromium consisted of addition of 0.06 to all values of f_{Fe} producing a change of less than 1% in R.

B. Comparison of calculated and observed R ratios showing effect of corrections.

Ratio		Calculated Fe and Cr scattering only	Calculated including Carbon correction	Observed Value
$\frac{R_{\gamma(311)}}{R_{\gamma(220)}}$	=	1.55	1.43	1.21
$\frac{R_{\alpha(211)}}{R_{\alpha(200)}}$	=	2.28	2.20	1.95

IV DISCUSSION AND CONCLUSIONS

Despite the uncertainties involved in the calculation of the percent austenite from x-ray data, the answers obtained may be regarded as acceptable but their accuracy does not necessarily establish the real austenite content. The fact does not, however, decrease the usefulness of the x-ray technique for determining retained austenite content. So long as reproducible results can be obtained, they may be used for correlations with physical properties even though their absolute values are of limited significance.

The results of this investigation show that the reproducibility of results obtained using the x-ray spectrometer is a function of the time used for a single determination.

For a given time per determination, the recorded pattern technique gives the most reproducible results. The recorded pattern results are in good agreement with those given by lineal analysis where the two methods are mutually applicable.

The automatic integration method cannot give results of the same accuracy as the recorded or point counted patterns because it permits only a linear background approximation between the line extremities. The choice of background points on either side of the line has an important influence on the results. The errors made using this method are most important in the range of austenite contents below 20 percent and above about 60 percent.

The point counted patterns give results of excellent reproducibility but require a longer time because a person must measure and record each point, plot the data, then measure the areas and convert their ratio to percent austenite.

Although the smallest austenite content measured in any of the samples used was about 3%, the method is capable of detecting amounts of austenite as small as 0.5%. The lower limit of the method is determined by the stability of the tube power output. With a highly stabilized tube output, 0.5% austenite could be measured with a good reproducibility in the same time.

The outstanding advantage of the spectrometer technique is that the time required to detect and measure amounts of retained austenite is small and is substantially independent of the amount present in the sample.

V SUGGESTIONS FOR FUTURE WORK

A series of samples might be prepared containing austenite contents varying in the widest range obtainable in a steel of a given composition. Retained austenite determinations made on the specimens as quenched and after darkening for lineal analysis could be compared with results from lineal analysis. A plot of the x-ray results as percent austenite versus the ratio $\frac{{}^{E}\alpha(200)}{{}^{E}\gamma(220)}$ should give a curve conforming to the equation

$$\% \gamma = \frac{(100 - \text{vol. \% carbides})}{1 + \left[\frac{{}^{E}\alpha(200)}{{}^{E}\gamma(220)} \cdot \frac{{}^{R}\gamma(220)}{{}^{R}\alpha(200)}\right]}$$

From such a plot, the real accuracy of the R values could be evaluated and the absolute accuracy of the method could be obtained.

APPENDIX I

Calculation of R Values for Chromium and Cobalt K_α Radiations

Line	%C	$\frac{1000}{v_\alpha^2}$	$\lvert F_{(hkl)}\rvert^2$	p	L.P.	R	R_C
			Cr K_α = 2.2863 kX				
α(200)	1.00	1.71	621	6	2.81	17.9	18.6
	0.80	1.74	620	6	2.81	18.2	18.7
	0.45	1.77	619	6	2.81	18.5	18.8
	0.25	1.79	617	6	2.81	18.6	18.7
γ(220)	1.00	.461	2116	12	3.91	45.8	47.4
	0.80	.471	2116	12	3.95	47.2	48.6
	0.45	.478	2116	12	4.04	49.0	49.6
			Co K_α = 1.7866 kX				
α(200)	1.00	1.71	450	6	3.46	16.0	16.7
α(211)	1.00	1.71	324	24	2.74	36.55	36.55
γ(220)	1.00	.461	1493	12	2.83	23.4	24.2
γ(311)	1.00	.461	1118	24	2.93	36.2	34.8

The R values for chromium radiation were based on iron scattering only, because at least 10 atom percent of chromium is required to change f_{alloy} by one percent at the position of the γ(200) line where the difference between f_{Cr} and f_{Fe} is greatest. The R values for cobalt radiation

APPENDIX I
(continued)

were calculated including the effect of chromium (which meant just less than a one percent increase in f_{Fe}). The R_C values for both radiations include the scattering of carbon as well as that of iron and chromium assuming that the carbon atoms occupy the tetrahedral positions in the martensite. The positions of carbon in martensite are not known with certainty and the results are of interest only as an order of magnitude approximation.

APPENDIX II

From Figure 11, Page 67, substitution of two degrees for α when the four degree divergence slit is used gives the following variation in diffracting volume, V, with 2θ for a unit path length (2x):

2θ Degrees	V (Arbitrary Volume Units)
50	1192
60	1189
80	1188
100	1188
120	1187
140	1187
160	1187

Thus, for all practical purposes, the absorption factor is the same for all lines provided that the irradiated area never extends beyond the edges of one flat surface of the sample. Since the lines are considered only as ratios, the absorption factor A may be considered unity for the range of 2θ used on the spectrometer.

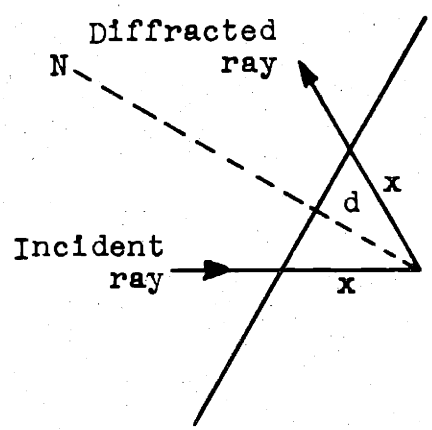

For any path length, 2x :

$d = x(\sin\theta)$

and the volume diffracting = V

$V = d(A+B) \cong$ constant

(See next page)

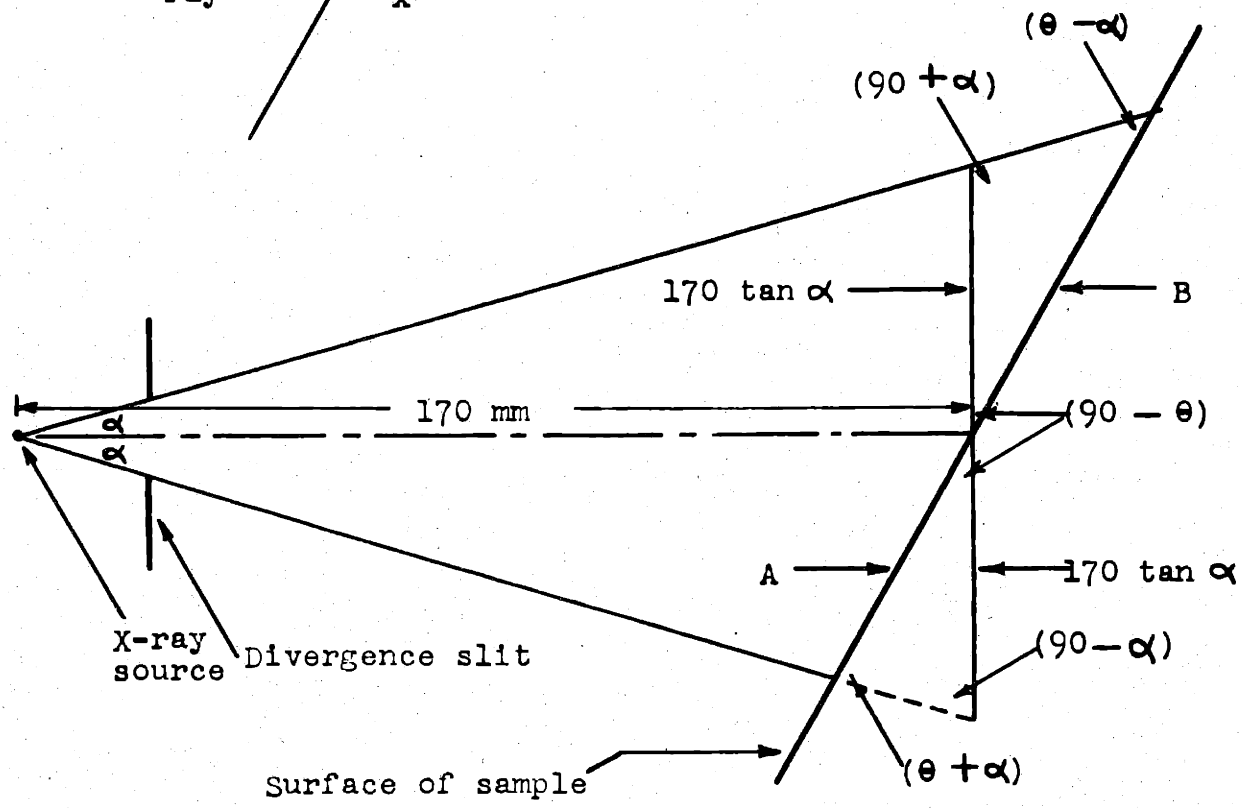

$$\frac{A}{\sin(90-\alpha)} = \frac{170\tan\alpha}{\sin(\theta+\alpha)} \; ; \quad \frac{B}{\sin(90+\alpha)} = \frac{170\tan\alpha}{\sin(\theta-\alpha)}$$

$$A = \frac{170\tan\alpha\cos\alpha}{\sin(\theta+\alpha)} ; \quad B = \frac{170\tan\alpha\cos\alpha}{\sin(\theta-\alpha)}$$

$$A + B = 170\tan\alpha\cos\alpha\left[\frac{1}{\sin(\theta+\alpha)} + \frac{1}{\sin(\theta-\alpha)}\right]$$

$$A \quad B = 170\sin\alpha \qquad (\qquad " \qquad)$$

Figure 11 Derivation of the Absorption Factor for the X-ray Spectrometer

BIBLIOGRAPHY

1. B. L. Averbach, L. S. Castleman and M. Cohen, "Measurement of Retained Austenite in Carbon Steels", Trans. ASM 42 (1950) 112.
2. B. L. Averbach, "Dimensional Changes in Hardened Gage Steels", Sc.D. Thesis, Department of Metallurgy, M.I.T., September 1947.
3. B. L. Averbach and M. Cohen, "X-ray Determination of Retained Austenite by Integrated Intensities", Trans. A.I.M.E., 176, (1948) 401.
4. R. T. Howard and M. Cohen, "Quantitative Metallography by Point-counting and Lineal Analysis", Trans. A.I.M.E. 172 (1947) 413.
5. J. W. Fitzwilliam, "X-ray Study of Order in Binary Systems", Ph.D. Thesis, Department of Physics, M.I.T. June 1947.
6. L. Mager, "X-ray Determination of Retained Austenite in Chromium Steel by Integrated Intensities", S.B. Thesis, Department of Physics, M.I.T., May 1950.

7. A. Taylor, An Introduction to X-ray Metallography, Chapman and Hall Ltd., London (1945)

8. R. W. James, The Optical Principles of the Diffraction of X-rays, G. Bell and Sons, Ltd., London (1948) p. 25.

9. K. H. Jack, "Structural Transformations in the Tempering of High Carbon Martensitic Steels", J. Iron and Steel Inst., 169 (1951) 26.

10. Smoluchowski, Mayer and Weyl, Phase Transformation in Solids, John Wiley and Sons, Inc., New York (1951) p. 590.

11. W. J. Harris and M. Cohen, "Stabilization of the Austenite-Martensite Transformation", T.P. 2446, Metals Technology, September 1948.

12. Personal communication with E. S. Rowland, Timken Roller Bearing Co., Canton, Ohio